Journal of Mechanical Engineering and Manufacturing
https://www.sciltp.com/journals/jmem

Article

Speed Vibrational Zones and Macro-Relief Formation of Machined Surfaces of Thin-Walled Structures under End Milling

Mykhaylo Frolov [1,*], Sergey Dyadya [2], Serhiy Tanchenko [1] and Viktoriia Shtankevych [1]

[1] Metal Cutting Machines and Tools Department, Mechanical Engineering Faculty, Zaporizhzhia Polytechnic National University, 69063 Zaporizhzhia, Ukraine
[2] Production Engineering Department, Mechanical Engineering Faculty, Zaporizhzhia Polytechnic National University, 69063 Zaporizhzhia, Ukraine
* Correspondence: mfrolov@zp.edu.ua; Tel.: +380-50-570-25-08

How To Cite: Frolov, M.; Dyadya, S.; Tanchenko, S.; et al. Speed Vibrational Zones and Macro-Relief Formation of Machined Surfaces of Thin-Walled Structures under End Milling. *Journal of Mechanical Engineering and Manufacturing* **2026**. https://doi.org/10.53941/jmem.2026.100020

Received: 3 February 2026
Revised: 27 February 2026
Accepted: 4 March 2026
Published: 28 April 2026

Abstract: The use of thin-walled structures and assemblies in high-tech industries such as aerospace, energy, defense, etc. solves many technical problems related to weight and size reduction, but also creates new ones. The machining of such structures is a challenge for industry, as they do not have sufficient rigidity to ensure dimensional accuracy and macro-relief requirements. The main factor affecting the quality of the machined surface is the vibrations that occur during machining, and a significant amount of research is devoted to mitigating their impact. This work is devoted to the formation of the macro-relief of the machined surface during end milling of thin-walled structures. The work shows that the cutting speed significantly affects the nature of vibrations, the patterns, and the mechanism of regular macro-relief formation. This is explained by belonging to one of the speed vibrational zones. The paper also considers the influence of the type of milling—down-cut and up-cut—on the formation of macro-relief and provides practical recommendations on the conditions for their application. The novelty of the study is in combining two approaches to zoning machining conditions and, accordingly, analysing vibration phenomena during the machining of thin-walled structures based on the Defining Ratio and using Stability Lobe Diagrams. Such a combination is possible for conditions in which Attendant Free Vibrations does not apply. As a criterion for selecting the conditions and type of machining, it is proposed to use the phase coefficient, which characterises the transition from the damped natural vibrations of the part to the cutting period of the next milling cutter tooth, which should significantly simplify the selection process. The article also formulates the direction of further research, which will contribute to solving the current production problem.

Keywords: down-cut milling; up-cut milling; surface topography; attendant free vibration; waviness; phase coefficient; defining ratio

1. Introduction

The development of such high-tech industries as aircraft and rocket manufacturing, satellite systems, and power units is associated with the need to reduce the weight of equipment while maintaining its reliability and rigidity. To a large extent, as noted in the works of [1–3], this goal is achieved by using thin-walled structures (elements) made of titanium, nickel, and aluminium alloys, stainless and structural steels. Such structures include: skin panels, stringers, frames, ribs, turbine blades, shells, etc. [2]. One of the existing classifications according to

which structures are classified as thin-walled is based on the ratio of the wall thickness (h) to the shorter side (p). If the ratio is within the range $1/100 \leq h/p \leq 1/5$, then such a structure is classified as thin-walled (TWS) [2]. The most common method of machining such structures is milling [2,3], which is a challenging task for production. The low rigidity of TWS leads to vibrations, which significantly affect the micro- and macro-relief of the machined surface, its deformation, and residual stresses. The regular macro-relief (which will henceforth be referred to as macro-relief) of the machined surface or its topography is formed in the form of waviness with a height W_z and a pitch S_w. According to Zablotskyi et al. [4], the presence of waviness is even more critical than roughness for many thin-walled structures. For example, in gas turbines, whose components operate at extreme temperatures and rotational speeds, the presence of waviness can lead to disruption of gas flow, resulting in increased vibrations and, as a consequence, the appearance of fatigue cracks, as well as a decrease in turbine efficiency. According to [5–7], the permissible waviness for gas turbines is usually set at 0.05 mm or less.

Despite a significant number of publications on TWS machining and the use of various means of vibration control, including artificial intelligence, as noted in the analysis by [8,9], the study of the formation of the topography of the machined surface remains relevant.

Therefore, the purpose of this article is to study the conditions for the occurrence of waviness during TWS milling and the trends that reflect the relationship between macro-relief parameters and the nature and character of TWS vibrations in the context of ensuring fairly strict tolerances for waviness height.

2. Literature Review

A detailed study of the influence of radial and axial cutting depth, as well as tool geometry, on the deformation and waviness of thin-walled parts is presented in the work by Kurpiel et al. [2]. The study was conducted at constant cutting speed and feed rate, and the design of the study is actually a ½ replica of a full factorial experiment 2^3. The author obtained the greatest waviness at the maximum axial and minimum radial cutting depth. However, this approach, on the one hand, does not provide an unconfounded estimate of the factors, and on the other hand, does not contain an analysis of the vibration component and the influence of cutting speed and feed rate on waviness, which, according to Dyadya et al. [10,11], have the most significant impact on it. Similar conclusions about the effect of cutting conditions are presented in the work by Kouahla et al. [12]. Based on Taguchi's analysis, the paper shows that cutting speed has a major impact (around 31%) on vibrations and the formation of the machined surface. Feed rate ranks second with an impact of 23%. The work by Wang et al. [13] analyzes the effect of cutting force on vibrations and feed rates on cutting force. However, the effect of cutting speed on cutting force is not considered. The importance of cutting force prediction in the context of its effects on vibration is noted by Zhao et al. [14], for which a model is developed for a tool with complex geometry, but the analysis of the effects of cutting conditions is lacking in the work. The study [15] by Dongre et al. highlights the significant impact of cutting speed on vibration phenomena and, as a result, on the quality of the machined surface, but through its influence on tool wear.

The works of Ozoegwu [16], Yi et al. [17], and the study by Kononenko et al. [18], noting the influence of vibrations on the quality of the machined surface of TWS, do not analyze the nature and method of vibrations from the position of their influence on the machining result. The influence of vibrations exclusively on surface roughness for its monitoring and without connection to macro-relief is also considered in the paper by Abebe and Gopal [19]. The result obtained in [16] may indirectly indicate the contrasting nature of the effect of conventional and climb end milling on the vibration component and, consequently, on the waviness of the machined surface.

Sedehi et al. [20] examine the effect of up-cut and down-cut milling on the mechanical properties of titanium alloy, its corrosion resistance, and wear resistance in the context of biomedical applications. Explaining the achievement of 14% increase in hardness and a significant increase in corrosion resistance after up-cut milling, 38–44% increase in wear resistance for both milling methods by an increase in dislocation density, the authors do not analyze the effect of the milling method on the micro- and macro-relief of the machined surface.

Hou et al. [3] as well as Ciecielag et al. [21] consider the cutting forces as the sources of chatter generation during the milling process, which, due to the low rigidity of TWS, lead to poor dimensional accuracy and surface roughness. The issue of assuring dimensional accuracy, namely the accuracy of the machined thin-walled part thickness, is also considered in the article by Lassila et al. [22] by choosing milling strategies.

A study by Wang et al. [23] develop dynamic model using the Stability Lobe Diagram (SLD) that provides adequate prediction of stable milling conditions. However, all the above works do not analyse either the milling method or the vibration component, including the mechanisms of macro-relief formation, as well as the differences between down-cut and up-cut milling, including comprehensive literature analyses by [8,24]. Regarding the latter, this issue has been studied in sufficient detail for milling parts that are not thin-walled, as in the work of

McClements & Tewolde [25]. At the same time, as noted in the work of Li et al. [26], there are fundamental differences in the milling of TWS.

As noted in [25], up-cut or conventional milling is a machining process in which the milling cutter rotates opposite the direction of the feed, so chips are formed from thin to thick, ensuring more stable cutting conditions and reducing vibration, minimising the risk of tool damage or part displacement. Therefore, for parts sensitive to vibration, up-cut milling has advantages.

The disadvantages of conventional milling include a lower quality of the machined surface, since machining actually starts from zero thickness, where there is no cutting process as such, but rather the friction of the cutting tool against the machined surface. This is characterised by increased heat generation and an upward force pushing the workpiece apart from the cutter, which contributes to accelerated tool wear, causes thermal and mechanical deformation of the tool and workpiece, resulting in reduced dimensional accuracy.

Down-cut milling, also called climb milling, is a machining process where the cutter and the workpiece both move in the same direction when cutting. This makes the chip start thick and then get thinner. This technique provides a more uniform machined surface, extends tool life due to reduced heat emission, including increased heat dissipation in the chips [25], but requires more reliable clamping of the part to overcome the pulling component of the cutting force that tends to shift the part from its clamping position. On the other hand, the downward component of the cutting force helps to stabilise the workpiece during cutting and reduce vibrations. This reduces the probability of deflection, particularly while machining thinner or more flexible materials. With reduced cutting opposition and enhanced chip removal, climb milling makes it possible to achieve higher feed rates and higher machining speeds without negatively impacting tool life or surface quality.

However, some disadvantages should also be considered. The tool tends to draw the workpiece towards itself, and if the machine has some kind of backlash, this can result in inaccurate dimensions or surface finish of the milled part, or even make the cutter "jump". Climb milling can also cause the workpiece to be pulled into the cutter, potentially resulting in movement or chatter. This is mainly a concern when working with thin workpieces. Contrary to the above conclusions, Li et al. [27] note better surface quality in up-cut milling than in down-cut milling, which is confirmed by both geometric analysis and experimental studies.

Understanding the mechanism of vibration and macro-relief formation allows zoning of milling conditions, one of the key factors of which is the milling cutter rotation frequency or cutting speed. The choice of a combination of cutting speed and radial cutting depth that ensures the stability of the cutting process also underlies the above-mentioned SLD. Zoning according to Munoa et al. [28] is based on the ratio of natural (f_n, Hz) and exciting (f_z, Hz) frequencies (see Equation (1)), which is used in combination with SLD. Exciting vibrations are the frequency of the cutter flute passing, which depends on its rotation frequency n (rpm).

$$k = \frac{f_n}{f_z} = \frac{60 f_n}{z_0\, n} \tag{1}$$

Here, z_0 is the number of cutter flutes.

Depending on the value of k, there are four SLD zones:

- Zone A ($k > 10$)—process damping zone. Here, a high degree of stability is achieved due to the friction of the rear surface of the flute against the wavy surface. The lower the spindle speed in this zone, the higher the stability limit.
- Zone B ($3 < k < 10$)—intermediate zone. The stability limit is close to the absolute stability limit of the entire spindle rotation frequency range. This is especially true for high degrees of damping.
- Zone C ($0.5 < k < 3$)—high-speed zone. In this zone, stability can be significantly increased by selecting a spindle speed that falls within one of the stability pockets.
- Zone D ($k < 0.5$)—ultra-high-speed zone. Cutting stability increases at higher cutting speeds. The limiting factor is the spindle power in combination with the specific type of vibration.

However, such zoning has little to do with the cutting process itself, since the natural frequency is a characteristic of the workpiece and, from this point of view, is only indirectly related to the cutting process [10]. The article by Vnukov et al. [29] considers another zoning principle—the defining ratio (DR), which is defined as the ratio of the cutting time t_c to the period of natural vibrations T_n—Equation (2). The zones defined in this way are characterised as speed vibrational:

$$DR = \frac{t_c}{T_n} = t_c f_n \tag{2}$$

Zoning works like this:

- Zone 1 ($DR > 10$). Characterised by low rotation frequencies and low productivity. The micro-relief is really bad due to the significant lapping. No waviness is observed.
- Zone 2 ($7 < DR < 10$). Milling is still unproductive. The surface quality associated with microgeometry improves, but slight waviness appears.
- Zone 3 ($1 < DR < 7$). At the initial stage of the cutting process, specific vibrations with an amplitude of more than 0.02 mm appear. The specificity of these vibrations is as follows: they occur exclusively during cutting time and have a distinct first wave. According to the research presented in [10,11], this first wave is the trigger for regenerative vibrations and the formation of macro-relief. That is why significant waviness is observed in this zone. These vibrations are defined in [10,11,25] as attending free vibrations (AFV).
- Zone 4 ($DR < 1$, $t_{is} > T_n$). Refers to high-speed milling, where idle time (t_{is}) is higher than the period of natural vibrations (T_n). The cutting time becomes significantly shorter than the period of natural vibrations. AFV are not observed. According to [29], forced and natural vibrations occur, and there is no observed effect of vibrations on the macro-relief of the machined surface.
- Zone 5. ($DR < 1$, $t_{is} < T_n$). Cutting in this speed zone, according to [29], does not differ from Zone 4 in terms of its characteristics and results, except that the idle time, is less than the period of natural vibrations. This fact is also noted in the work of Germashev et al. [30].

The authors of [28] indirectly refer to this zoning, comparing the cutting time and the period of natural vibration in the descriptive part of their work. Contradictions between the zoning approaches proposed in works [28,29] can be resolved by considering zones A–D according to [28] within zones 4 and 5 according to [29], where the cutting time is very short, and AFV is not available. However, if so, machining in speed vibrational zones 4 and 5 cannot guarantee the absence of waviness, since the cutting conditions must correspond to one of the SLD "stability pockets" for zones A, B, C and D. In other words, under certain conditions, waviness may also be formed in the 4th and 5th speed zones, contrary to statement of work [29]. Furthermore, work [28] notes that each machining mode has a range of spindle rotation frequencies where chatter occurs.

The above analysis confirms the relevance of the problem of TWE machining and ensuring their proper quality. This is also evidenced by the data presented by Frolov et al. in [31], which notes a steady increase in publications on this topic. However, it should be noted that the analyzed publications focus mainly on approaches to ensuring the specified surface roughness (microrelief) and geometric accuracy. At the same time, the problem of ensuring proper regular macro-relief, which is determined by vibration phenomena during the milling process, is practically not studied. At the same time, based on the analyzed works, it is difficult to identify connection between vibrations and cutting conditions in general and cutting speed in particular that have a crucial impact on the macro-relief formation processes. Taking into account the zoning of milling conditions, the key component of which is the cutting speed, which determines changes in the character of vibration phenomena, the tasks to be solved in this work are as follows:

- To study the patterns of transition from the third to the fourth vibrational zone with regard to vibrations that directly attend the cutting process, forming a regular macro-relief of the machined surface, and subsequently exist during idle running.
- To study and find out conditions for the absence or presence of waviness during end milling of TWS in the 4th vibrational speed zone.
- Research the influence of the milling method—down-cut and up-cut—on the formation of regular macro-relief during end milling of TWS in the 4th speed zone.

3. Methodology

Based on the literature review and the research objective, since cutting speed is a physically and theoretically justified key factor related to the formation of macro-relief [10], the spindle rotation frequency (cutting speed) is selected as the main variable parameter. In addition, the rotational speed determines the excitation frequency, affects the ratio of the cutting time to the natural vibration period (Defining Ratio), ensures the transition between speed vibrational zones, and forms the basis for SLD construction as per [28]. The rotational frequency range is selected to ensure representativeness with respect to the entire physical pattern under study, namely: covering the $DR > 1$ (3rd zone), to fix the transition region ($DR \approx 1$), to investigate the behaviour of the system in the 4th speed zone ($DR < 1$), to ensure that it falls within different SLD regions (A–D according to classification of [28]). Two values of radial cutting depth (0.1 and 0.3 mm) were taken for the studies in order to analyse vibration effects at low force loads and assess the stability of the identified patterns as the dynamic impact increases. The use of a single-flute milling cutter eliminates the overlapping of flute marks and simplifies the interpretation of the macro-relief wave structure.

The tests for the TWS milling process research are based on the single-factor approach ensuring analysis of the cutting speed influence without confounding factors and maintaining the results' comparability with previously published works on AFV [10,11,32].

The samples are machined at MC6104-13WK CNC milling machine (Shenyang Machine Tool Co., Ltd., Shenyang, China) using a special setup that is described in detail at [10,11]. It is equipped with an electric contact device for registering the start and the end of cutting time. The sample displacements are measured by the proximeter of mod. XS4P12AB110 (Schneider Electric SE, Rueil-Malmaison, France) switching frequency 2000 Hz). To record and store data obtained, the L-Graph software (L-Card, Moscow, Russia) is used. For data in the form of oscillogram analysis—Power-Graph software. The general view of the testing installation is shown in Figure 1a. The special milling cutters, including those that have changeable flute number and helical angle are presented in Figure 1b. Samples of the size 50 × 25 × 4 (Figure 1c) are mounted on a special support with changeable elastic characteristics.

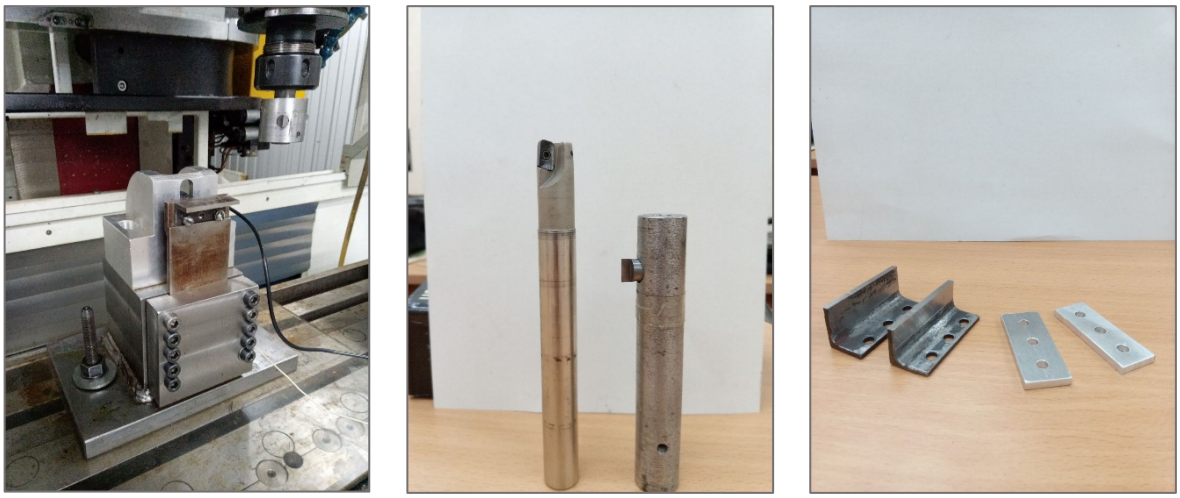

(**a**) (**b**) (**c**)

Figure 1. Testing installation (**a**); special milling cutters (**b**); and samples (**c**).

The research parameters are given in Table 1, and the variable factors are listed in Table 2.

Table 1. Research parameters.

No	Title	Value
1	Material of the sample	Steel 3 (EU analogue Fe37-3FN): R_m410 MPa, HB170 Chemical composition: C 0.14–0.22% Si 0.15–0.3% Mn 0.4–0.64%
2	Material of the cutting element	BK10 Carbide Grain size: 2–4 µm Chemical composition: Cobalt (Co) ~8% Tungsten carbide (WC) ~92%
3	The milling cutter helix angle—ω^0	0
4	Number of milling cutter flutes z_0	1
5	Axial depth of cut a_p, mm	4
6	Feed per flute, S_z, mm/f	0.1

Table 2. Variable factors.

Radial Depth of Cut a_r, mm	**0.1**	**0.3**
Rated cutter rotational speed, rpm	600, 1200, 1800, 2400, 3000, 6000, 8000	800, 1500, 2500, 4000, 6000
The natural vibration frequency of the samples f_n, Hz (specified for each one)	463.87, 488.28	415.04
The diameter of the milling cutter D_0, mm	16, 28	16

The characteristics of machined surface waviness are recorded by a profilometer-profilograph Kalibr 170311 (JSC "Kalibr", Moscow, Russia) with the following characteristics: probe–diamond needle with a tip radius of 10 ± 2.5 μm; height measurement range 0.02 μm–500 μm; maximum track length 50 mm.

Before conducting a test series, the following procedures were performed: The XS4P12AB110 proxymeter (Schneider Electric SE, Rueil-Malmaison, France) was tested for sensitivity and linearity of response by moving a reference calibration plate with a known displacement (deviation no more then ±2.0%); the recording system (L-Graph, Power-Graph (L-Card, Moscow, Russia)) was tested for absence of zero drift (deviation no more then ±0.65 μm); the Kalibr 170311 profilometer-profilograph was calibrated against a reference roughness samples (deviation no more then ±4.0%); the spindle rotation speed was controlled by digital laser tachometer and built-in CNC system of the milling machine (deviation no more then ±1.5%).

To exclude the influence of uncontrolled factors, the following conditions were met: all experiments were conducted on the same machine; the same batch of material was used; the geometry and method of fixing the samples were identical in all tests; the natural frequency of each sample—f_n (Hz) was defined by analysis of the corresponding oscillogram, using the above software with Short-Time Fourier Transform [28]; the tool was checked for signs of wear so it could be replaced if there were any; each mode was performed as a series of repetitions.

A statistical assessment of the effects of cutting speed on the factors under investigation is carried out by evaluating the presence of a significant difference between two consecutive mean values using comparison of means by Student's *t*-test with Cochran-Cox adjustment. The calculation formulas for small samples ($n_i < 30$) are given in Table 3 [32].

Table 3. Calculation formulas for the Cochran-Cox averages comparing method.

Calculated Value of the *t*-Test	Adjusted Degree of Freedom
$t_{i,i+1} = \frac{1}{\sqrt{\frac{S_i^2}{n_i} + \frac{S_{i+1}^2}{n_{i+1}}}} (\lvert \bar{Y}_i - \bar{Y}_{i+1} \rvert)$	$\nu = \left\lfloor \frac{[S_i^2/n_i + S_{i+1}^2/n_{i+1}]^2}{\frac{(S_i^2/n_i)^2}{n_i - 1} + \frac{(S_{i+1}^2/n_{i+1})^2}{n_{i+1} - 1}} \right\rfloor$

Where S_i^2 is the variance of the respective independent experiments; Y_i is the mean value of the measured quantity in the respective independent experiments; n_i is the number of replications in the respective independent experiment; $t'_{q,\nu}$—critical value of the *t*-test for confidence probability *q* and *v* degrees of freedom. The hypothesis of equality of means is not rejected if the condition (3) is met:

$$t_{i,i+1} \leq t'_{q,\nu} \tag{3}$$

The belonging of the conditions under consideration to a particular vibrational zone was determined by the value of the *DR* index as per Equation (2), which is accompanied by the presence or absence of specific and distinguishable attendant free vibrations (AFV), described in detail in [10,11,32].

4. Results

4.1. The Influence of Cutting Speed on the Forced Vibrations Characteristics that Affect the Machined Surface's Regular Macro-Relief Formation

A visual distribution by speed vibration zone according to [28] and [29], taking into account the ащгкequency ranges of samples for different cutter diameters D_o and milling methods, is shown in Figure 2. Here, it is proposed to consider zones according to classification [28] within Zone 4 according to classification [29], which eliminates the existing contradiction in conditions where AFVs do not act, and only the factors underlying zoning according to [28] remain—natural and exciting vibration frequencies.

To analyse processes in vibrational zones, it is essential to determine the cutting time and idle time—t_{is}. For the calculation of cutting time t_c, work [29] contains dependence (4)

$$t_c = \frac{30}{\pi \cdot n}\left[\cos^{-1}\left(1 - \frac{2a_r}{D_0}\right) + \frac{S_z}{D_o} + \frac{2 \cdot a_p \tan\omega}{D_0}\right] \tag{4}$$

The dependence does not differ for down-cut and up-cut milling. Accordingly, the idle time will be determined by Equation (5)

$$t_{is} = t_z - t_c \tag{5}$$

where t_z is the milling time per flute in seconds, determined by Equation (6):

$$t_z = \frac{1}{f_z} = \frac{60}{z_0 n} \tag{6}$$

A comparison between the experimentally obtained cutting times from the oscillogram and the calculated values shows a slightly overestimated calculated time for both down-cut (Figure 3a) and up-cut milling (Figure 3b). Regarding idle time, the significantly shorter cutting time has little impact on it, and the values differ by no more than 2.5%.

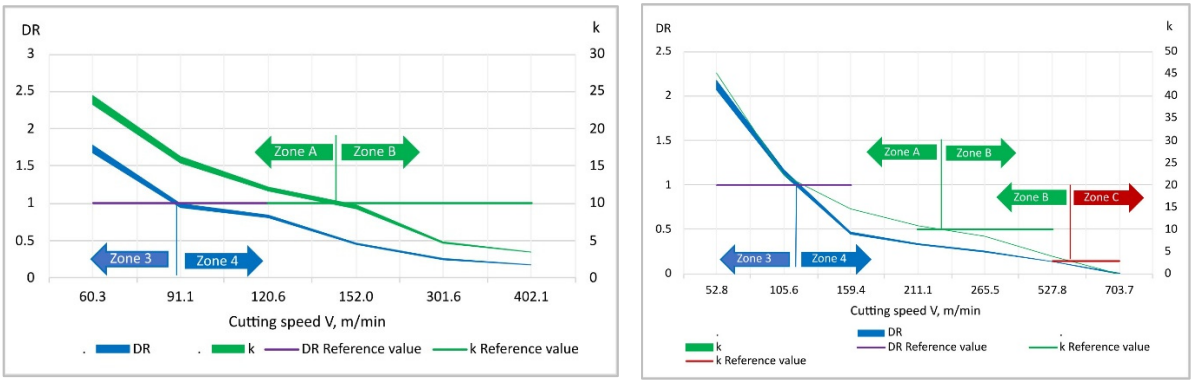

(**a**) (**b**)

Figure 2. Distribution by speed vibrational zones according to [28,29] zoning principles: (**a**) down-cut milling $D_0 = 16$; (**b**) up-cut milling $D_0 = 28$.

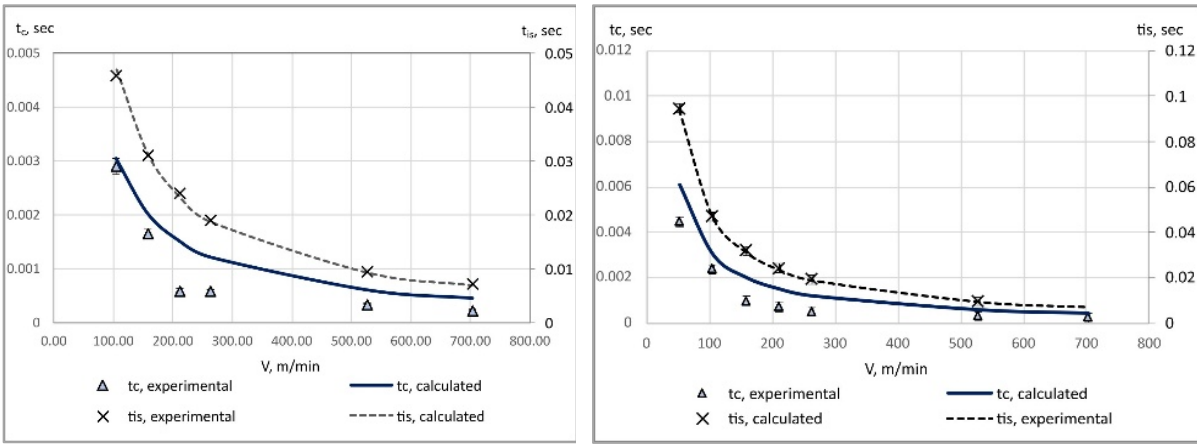

(**a**) (**b**)

Figure 3. Experimental and calculated values of cutting and idle times for down-cut (**a**) and up-cut (**b**) milling.

The factors determining machined surface macro-relief formation—height (W_z, mm) and waviness pitch (S_z, mm) in the 3rd speed vibrational zone according to [10,11] are, respectively, the deviation of the first AFV wave from the position of elastic equilibrium (EEP)—Δ (mm) and the wavelength—L_w (mm), which is related to the period T_w (sec) by the ratio (7), where V is the cutting speed, m/min.

$$L_w = T_w \frac{V}{60} \tag{7}$$

When shifting from 3 to 4 speed zones, AFVs decline, but the first wave remains quite noticeable (Figure 4). Therefore, the symbol Δ will be used to indicate the deviation of the first wave from EEP, regardless of whether it belongs to the specific speed vibrational zone.

Since the cutting time decreases and the wave period becomes greater than it, with the first and second half-periods differing from each other by 1.33...1.35 times for down-cut and by 1.07...1.16 times for up-cut milling, decreasing and increasing accordingly, to obtain comparable data, the dependence on the cutting speed of the half-periods of the first wave—τ_w is considered. Accordingly, the half-length of the first wave—λ_w is considered as well. The results of statistical analysis of significant differences in sequential half-period values for confidence probability $q = 0.95$ and the number of observations for each value $n_i = 20$ are presented in Tables 4 and 5 for up-cut and down-cut milling, respectively.

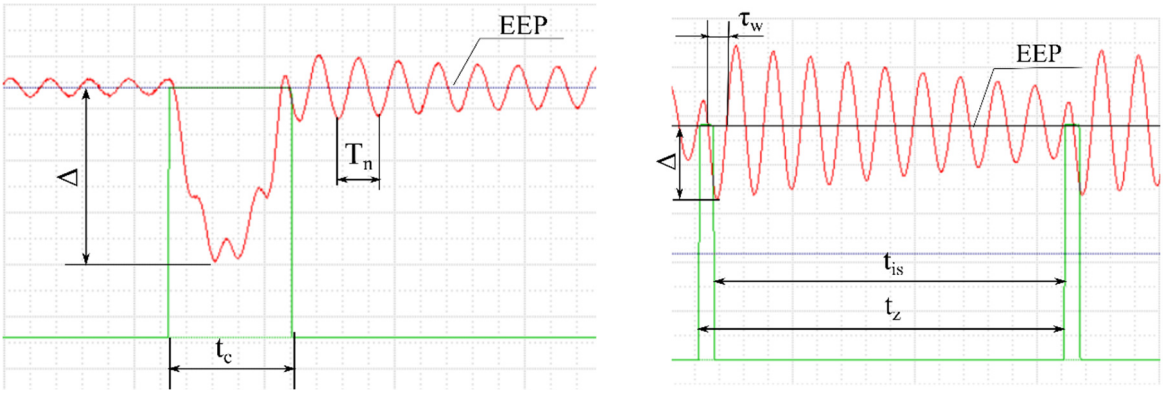

(**a**) (**b**)

Figure 4. Nature of vibrations during cutting in the 3rd (**a**) and 4th (**b**) speed vibrational zones.

Table 4. Assessment of the effectiveness of cutting speed on the half-wave length for down-cut milling. $D_0 = 28$.

V, m/min	Mean Value τ_w, mm	Variance S_i^2	Degrees of Freedom v	t-Test $t_{i,i+1}$	Critical Value $t'_{0.95,v}$	Confidence Interval Δ
105.6	0.00239	1.202×10^{-8}				±0.00005
161.0	0.00146	5.497×10^{-9}	33	31.608	1.692	±0.00004
211.1	0.00114	2.927×10^{-8}	25	7.678	1.708	±0.00009
265.5	0.00118	1.205×10^{-7}	27	0.424	1.703	±0.00018
527.8	0.00114	3.067×10^{-8}	28	0.460	1.701	±0.00009
703.7	0.00112	4.773×10^{-8}	36	0.283	1.688	±0.00011

Table 5. Assessment of the effectiveness of cutting speed on the half-wave length for down-cut milling. $D_0 = 28$.

V, m/min	Mean Value τ_w, mm	Variance S_i^2	Degrees of Freedom v	t-Test $t_{i,i+1}$	Critical Value $t'_{0.95,v}$	Confidence Interval Δ
52.8	0.00109	3.558×10^{-9}				±0.00002
105.6	0.00094	4.167×10^{-10}	23	9.682	1.713	±0.00001
161.0	0.00110	1.361×10^{-9}	29	15.986	1.699	±0.00001
211.1	0.00107	4.889×10^{-9}	29	1.450	1.699	±0.00003
265.5	0.00111	5.444×10^{-9}	37	1.627	1.687	±0.00003
527.8	0.00107	7.396×10^{-9}	36	1.342	1.688	±0.00003
703.7	0.00106	6.222×10^{-9}	37	0.106	1.687	±0.00003

With an increase in cutting speed, the half-period of the first wave decreases and in the 4th zone approaches the period of natural vibrations. This pattern remains the same for both down-cut (Figure 5a) and up-cut (Figure 5b) milling, and at cutting speeds above 150 m/min, the values of the half-periods become statistically indistinguishable from each other for both.

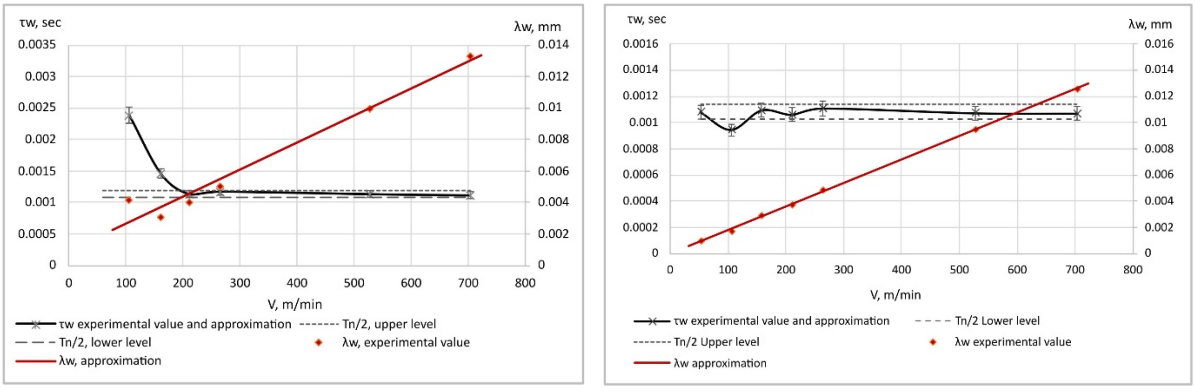

(**a**) (**b**)

Figure 5. Dependence of the first-wave half-period and half-length on cutting speed during down-cut $D_0 = 28$ (**a**) and up-cut $D_0 = 28$ (**b**) milling.

The nature of the influence of cutting speed on the height of the first wave deviation from EEP—Δ differs for the third and fourth zones, but does not differ for down-cut and up-cut milling. In Zone 3, in the considered

speed range, which is directly adjacent to Zone 4 ($1 < DR < 2$), the height of Δ increases, which does not contradict the results presented in [10]. When moving to Zone 4, it decreases. Both dependencies for both down-cut and up-cut milling are adequately approximated by linear dependencies, the graphs of which are shown in Figure 6. The height Δ for up-cut milling in this case is higher.

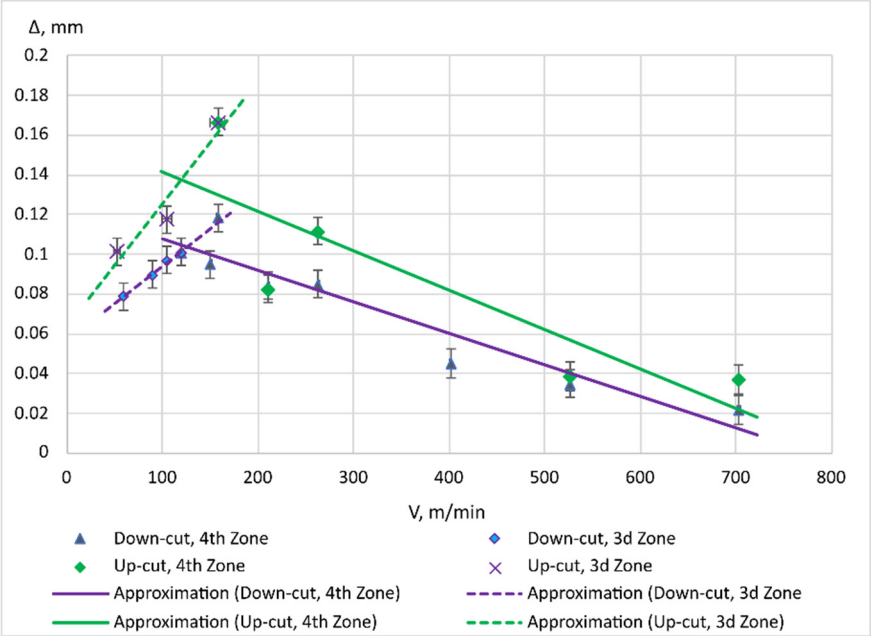

Figure 6. Dependence of the first wave height on cutting speed.

4.2. Transition from Natural Vibrations to Forced Ones in the 4th Vibrational Speed Zone

From the analysis of the transition patterns from the end of idle running with damped natural vibrations to the start of cutting by the next cutter flute (Figure 7) in the 4th vibrational speed zone, the following conclusions can be drawn:

- the formation of the first wave during down-cut milling begins at the moment of contact between the flute and the workpiece, which is natural since the flute cuts immediately to its full thickness (Figure 7a);
- the formation of the first wave during up-cut milling begins closer to the middle of the contact time, due to the start of cutting from zero thickness (Figure 7b);
- The transition from damped natural vibrations to the first wave of a new cutting period can begin as a continuation of the wave of damped natural vibrations (Figure 7a), when the phase of the latter φ at the moment of contact is within the range from 0 to $3/2 \times \pi$.
- the transition from damped natural vibrations to the first wave of a new cutting period may begin as a break in the wave of damped natural vibrations (Figure 7b), when the phase of the latter φ at the moment of contact is in the range from $3/2 \times \pi$ to $2 \times \pi$

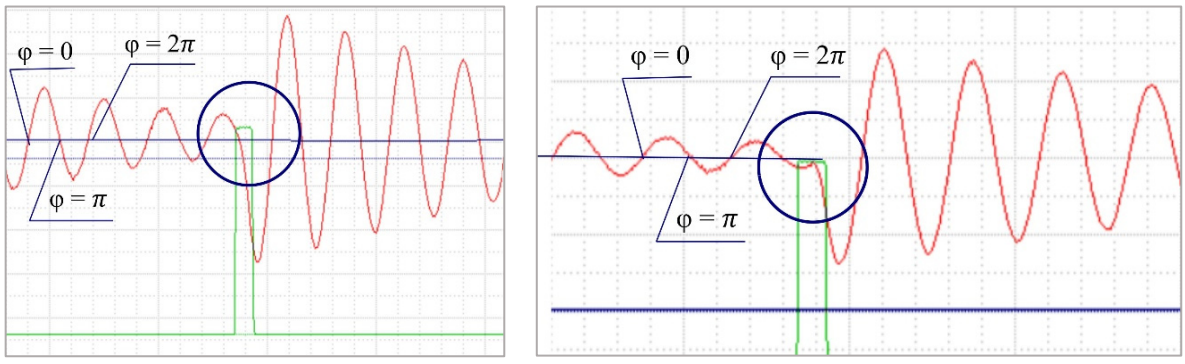

(**a**) (**b**)

Figure 7. Formation of the first wave of vibration during end milling: (**a**) start of cutting during down-cut milling; transition from natural vibrations to the wave of cutting start as a continuation; (**b**) start of cutting during up-cut milling; transition from natural vibrations to the wave of cutting start as a break.

The type of transition from damped natural vibrations to the first wave of a new cutting period in zone 4 depends on the phase of the residual number of waves m per period T_c (Equation (8)):

$$T_c = t_z - \frac{T_n}{2} \tag{8}$$

The phase of damped vibrations can be expressed in terms of the phase coefficient at π ($\varphi = \mu \times \pi$)—μ, which is determined by Equation (9):

$$\mu = 2(m - [m]) \tag{9}$$

where m is the number of waves that is determined by Equation (10) and $[m]$—integer part of m. Here and below, μ takes values from 0 to 2.

$$m = \frac{T_c}{T_n} \tag{10}$$

Alternatively, if the milling time and the period of natural vibrations are expressed in terms of the corresponding frequencies, the following expression (11) is obtained:

$$m = k - \frac{1}{2} \tag{11}$$

Or taking into account Equation (11), the phase coefficient in Equation (12) can be expressed as a fractional part of wave number (indicated in curly brackets).

$$\mu = 2\left\{k - \frac{1}{2}\right\} \tag{12}$$

Equation (12) demonstrates the relationship between zoning according to [28] and the 4th vibration speed zone according to [29].

4.3. Theoretical Justification

Vibrations during cutting occur in the form of harmonic oscillations [33], which are natural damped modes after the cutting process has stopped. The conditions for the machined surface macro-relief formation will depend on the superposition character of natural damped vibrations and forced ones caused specifically by the cutting process. Neglecting the change in amplitude during the last period of natural vibrations before the start of cutting by the next flute and taking into account Equation (8), the equation of natural vibrations can be written as follows (See Equation (13)):

$$f_n(t) = A_n \sin\left[\frac{2\pi}{T_n}t - \pi\right] \tag{13}$$

where A_n—amplitude of a natural vibration, mm; t—time in sec.

For forced vibrations caused by the cutting process and for time $t_1 \geq t$, the equation of harmonic oscillations is written as in Equation (14)

$$f_z(t_1) = -A_z \sin\left[\frac{2\pi}{T_z}(t_1 - t)\right] \tag{14}$$

where A_z—amplitude of a forced vibration during cutting time, mm; T_z—period of a forced vibration, sec. Considering the research results presented above, it can be accepted that: $T_z \approx T_n$.

The relationship between the energy of vibrations during cutting and the quality of the machined surface is direct and multi-component. The higher the proportion of energy transferred to the vibrational processes of the system, the more the micro- and macro-geometry parameters of the surface deteriorate [29]. Energy, in turn, is directly proportional to the square of the vibratory motion velocity.

The sum velocity will consist of the velocities of natural (V_n) and forced (V_z) vibrations. The vector equation of the sum velocity will look as follows (Equation (15)):

$$\vec{V_s} = \vec{V_n} + \vec{V_z} \tag{15}$$

If the components of Equation (15) are expressed in terms of unit vectors as shown in Equations (16) and (17):

$$\vec{V_n} = a_n\vec{i} + b_n\vec{j} \tag{16}$$

$$\vec{V_z} = a_z\vec{i} + b_z\vec{j} \tag{17}$$

then the modulus of the sum velocity will be determined as follows—Equation (18)

$$V_s = \sqrt{(a_n + a_z)^2 + (b_n + b_z)^2} \tag{18}$$

The vector Equations (16) and (17) components will be determined based on the derivatives of Equations (13) and (14), as shown in Equations (19)–(24).

$$a_n = \frac{1}{\sqrt{1 + (f_n'(t))^2}} \tag{19}$$

$$b_n = \frac{f_n'(t)}{\sqrt{1 + (f_n'(t))^2}} \tag{20}$$

$$a_z = \frac{1}{\sqrt{1 + (f_z'(t_1))^2}} \tag{21}$$

$$b_z = \frac{f_z'(t_1)}{\sqrt{1 + (f_z'(t_1))^2}} \tag{22}$$

$$f_n'(t) = 2\pi\frac{A_n}{T_n}cos\left[2\pi\frac{t}{T_n} - \pi\right] = 2\pi\frac{A_n}{T_n}cos\left[\pi\left(\frac{2t}{T_n} - 1\right)\right] \tag{23}$$

$$f_z'(t_1) = -2\pi\frac{A_z}{T_n}cos\left[\frac{2\pi}{T_n}(t_1 - t)\right] \tag{24}$$

It can be assumed that the forced vibrations begin at the start of the cutting process, i.e., at $t_1 = t$, so the velocity of the forced vibrations at this moment will be determined from Equation (24) as in Equation (25):

$$f_z'(t) = -2\pi\frac{A_z}{T_n} \tag{25}$$

In Equation (23), the expression in round brackets represents a phase coefficient, which is not limited here to the range from 0 to 2 (See Equation (26)):

$$\mu' = \frac{2t}{T_n} - 1 \tag{26}$$

The dependencies of the total velocity square on the phase coefficient μ ($\mu = \mu'$)—see Figure 8, constructed for arbitrary data (Figure 8a) and ones close to those under consideration (Figure 8b), show their similar nature, a characteristic feature of which is the presence of a minimum in the ranges close to 0–0.5 and 1.5–2. In the first range, the function increases, and in the second range, it decreases.

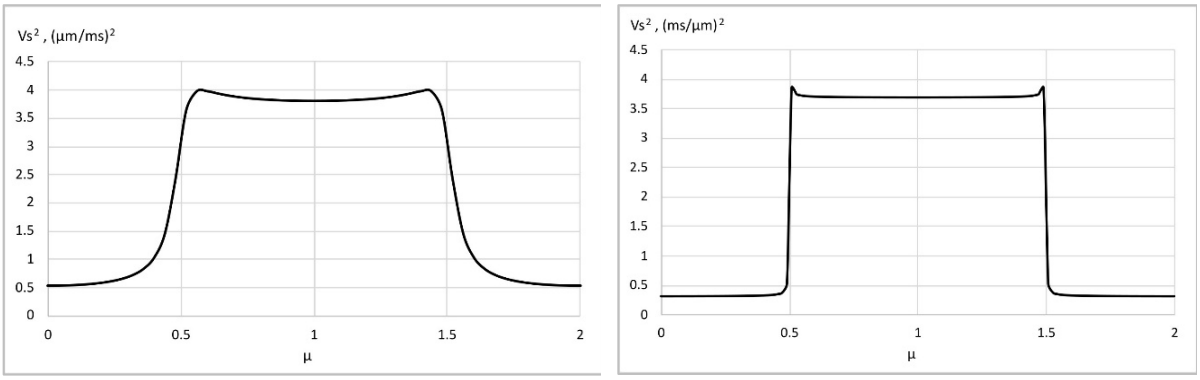

(**a**) (**b**)

Figure 8. Dependence of squared total velocity on phase coefficient: (**a**) $T_n = 50$ ms, $A_n = 50$ μn, $A_z = 100$ μm; (**b**) $T_n = 2.2$ ms, $A_n = 66$ μn, $A_z = 237$ μm.

Another factor that has a direct impact on vibrations is acceleration, which determines the force acting on an object, causing its deflection and, accordingly, affecting the parameters of micro- and macro-relief. A direct relationship between the quality of the machined surface and the applied force is indicated by a number of studies analysed in Section 2. The acceleration index (α) for analysis is taken as the ratio of the velocity increment (ΔVs) to the corresponding increments of time (Δt)—see Equation (27), constructed as a function of the corresponding phase coefficient μ:

$$\alpha = \frac{\Delta V_s}{\Delta t} \tag{27}$$

The dependency graphs are shown in Figure 9.

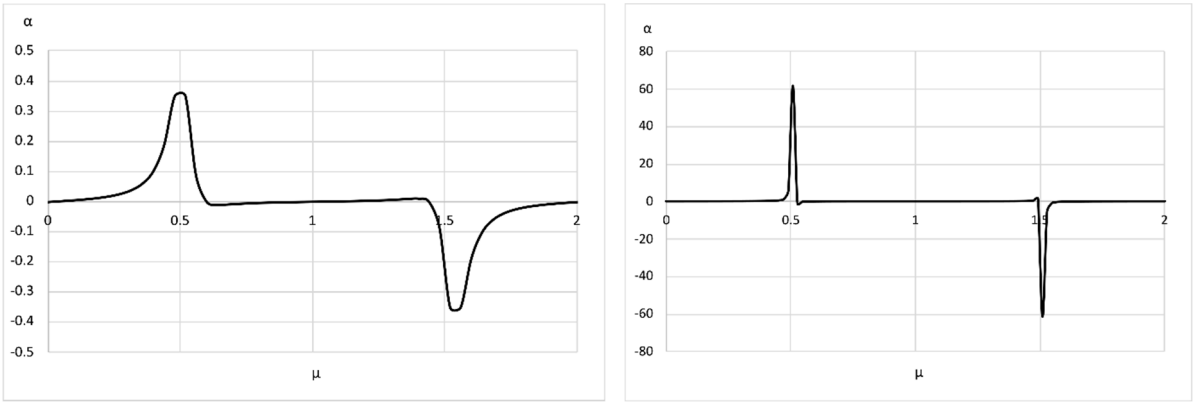

(**a**) (**b**)

Figure 9. Dependence of acceleration index on phase coefficient: (**a**) $T_n = 50$ ms, $A_n = 50$ μm, $A_z = 100$ μm; (**b**) $T_n = 2.2$ ms, $A_n = 66$ μm, $A_z = 237$ μm.

From a joint consideration of the dependencies in Figures 8 and 9, it is possible to hypothesize the existence of a range that is least favourable in terms of its effect on vibrations and, accordingly, the formation of the machined surface relief. This range is characterised by maximum total velocity and high acceleration values. The lower limit of the range corresponds to phase coefficient values of μ = 0.3...0.4, and the upper limit—μ = 1.4…1.5.

4. Discussion

Generalisation of the obtained data on the phase coefficient and wave height values demonstrates the relationship between them for both up-cut and down-cut milling. Diagrams for different cutter diameters D_0 and radial depth of cut 0.1 mm are shown in Figure 10. Figure 11 shows the same relations for a radial depth of 0.3 mm. The diagrams also display confidence intervals for regular waviness heights relative to their mean values for a confidence probability of q = 0.95 and the number of cases N = *12*, as well as the maximum of the measured values. The columns with horizontal hatching refer to the third vibrational speed zone (see Figure 2), and the patterns under consideration do not apply to these data, since the formation of macro-relief occurs under the influence of AFV [10,11,32], which are unavailable in Zone 4. The reference zone highlights the range of $\mu \approx 0.3 \ldots 1.45$ that is least favourable in terms of its impact on macro-relief formation.

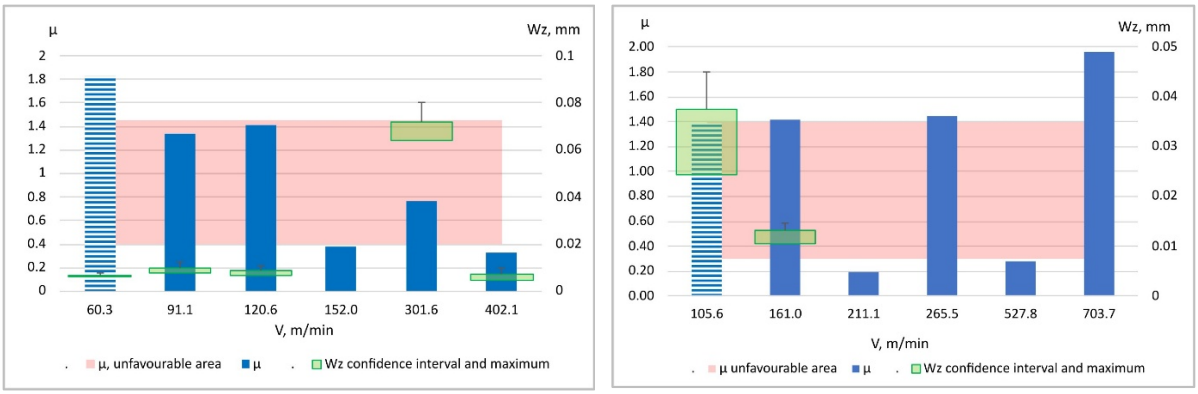

(**a**) (**b**)

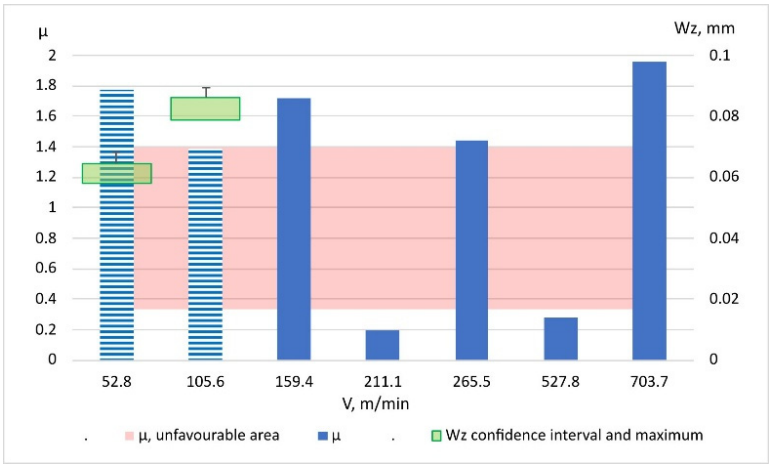

(**c**)

Figure 10. Diagrams of phase coefficient values for radial depth 0.1 mm: (**a**) Down-cut milling, $D_0 = 16$, $f_n = 488.28$Hz; (**b**) Down-cut milling, $D_0 = 28$, $f_n = 463.87$Hz; (**c**) Up-cut milling, $D_0 = 28$, $f_n = 463.87$Hz.

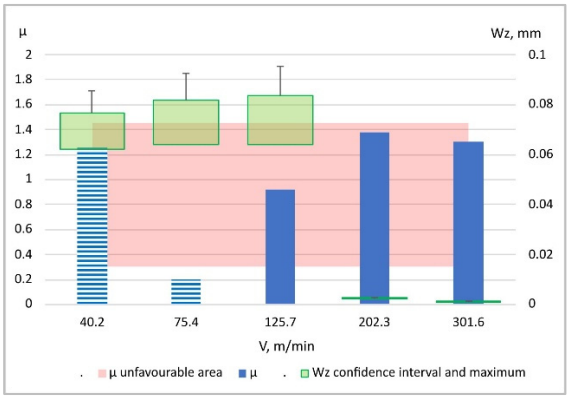

(**a**)

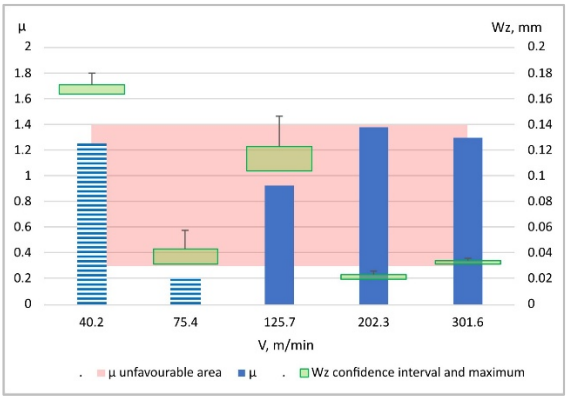

(**b**)

Figure 11. Diagrams of phase coefficient values for radial depth 0.3 mm, $D_0 = 16$, and $f_n = 415.04$ Hz: (**a**) Down-cut milling; (**b**) Up-cut milling.

As can be seen from the data presented, in the 4th vibrational speed zone, when the phase coefficient values are in the unfavourable range, waviness forms regardless of the radial cutting depth and the type of milling—down-cut or up-cut. For down-cut milling at radial depth of 0.1 mm, the waviness height varied from $W_z = 0.0078 \pm 0.0010$ for speed 91.1 m/min to $W_z = 0.0681 \pm 0.0040$ at cutting speed 301.6 m/min (Figure 10a,b). No regular macro-relief formation was observed during up-cut milling under these conditions (Figure 10c).

At a radial depth of 0.3 mm for down-cut milling, the minimum waviness height $W_z = 0.0011 \pm 0.0001$ was noted at a speed 301.6 m/min, and the maximum—$W_z = 0.0738 \pm 0.0097$ at a speed 125.7 m/min (Figure 11a). A similar result was observed for up-cut milling: the minimum height $W_z = 0.0213 \pm 0.0014$ was found at a speed of 202.3 m/min, and the maximum $W_z = 0.1134 \pm 0.0014$ at a speed of 125.7 m/min (Figure 11b).

Thus, it can be concluded that, as expected, in Zone 4 there may be areas of instability where waviness is significantly higher than at other speeds and other equal conditions, clearly exceeding the previously noted permissible limits. Under the conditions considered, instability zones were observed at phase coefficient values within the unfavourable range. As noted above, this is contrary to the findings of study [29] and therefore requires further exploration, since the described patterns were found for a wide range of cutting speeds but for a limited number of values of radial and axial cutting depth, feed rate, and physical characteristics of the material being machined. Based on this, the research should be continued by increasing the number of levels of conditions and parameters of the milling mode and taking into account their combinations.

Generalised data on the formation of waviness at different phase coefficients for down-cut and up-cut milling are given in Table 6, including the typical shape of regular macro-relief. The range of waviness height variation given in the table is calculated based on experimentally obtained average values and their confidence intervals.

Table 6. Macro-relief formation for the 4th vibrational speed zone.

$\varphi = \mu \times \pi$	Down-Cut Milling	Up-Cut Milling
$\mu \approx 0.3 \ldots 1.45$	$0.0010 \leq W_z \leq 0.0835$ 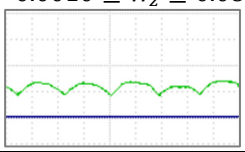	$0.0199 < W_z < 0.1148$ 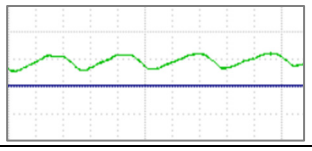
$0 \leq \mu < 0.3$ $1.45 < \mu \leq 2$	$0 \leq W_z \leq 0.0073$ 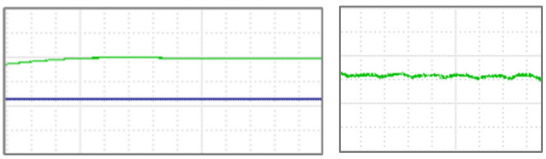	$W_z = 0$ 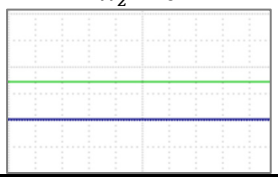

5. Conclusions

- The nature and regularities of vibration phenomena during TWS end milling depend on the milling conditions belonging to one of the five speed vibrational zones, which are determined by the ratio of the cutting time and the period (frequency) of the part's natural vibrations
- The most favorable in terms of the absence of waviness of the machined surface is the fourth speed vibrational zone, which refers to high-speed milling.
- The trends in the change of vibration characteristics during the end milling of TWS are the same for both down-cut and up-cut milling.
- The transition pattern from natural to forced vibrations can be assessed by the phase coefficient, which varies from 0 to 2.
- Theoretical analysis shows that, regardless of the amplitudes of natural and forced vibrations, there is a range of unfavourable phase coefficient values between approximately 0.3 and 1.45. This range is characterised by maximum total vibration velocity and acceleration.
- Under the observed conditions, the formation of regular macro-relief was noted in the 4th vibrational speed zone at phase coefficient values within the unfavourable range.
- For both down-cut and up-cut milling in the 4th vibrational speed zone, at certain speed values, sections of instability are observed, characterised by waviness height values exceeding the permissible limit and being 3 to 12 times higher than the heights at other speeds. Sections of instability correspond to phase coefficient values within the unfavourable range.
- Using the phase coefficient as a reference when selecting the cutting speed should potentially eliminate the choice of speed in the instability area where the waviness height is significantly higher than at other speeds and other equal conditions, as well as considerably simplify the selection procedure compared to SLD. However, since according to the theory underlying the design of SLD, instability areas are formed at certain combinations of cutting speed and axial depth, the conditions of TWS end milling require further study with a greater number of milling mode parameter levels, taking into account their combinations.

Author Contributions

M.F. and S.D.: conceptualisation, methodology, writing—original draft preparation, supervision; M.F.: statistics; S.T.: investigation, test, reviewing. V.S.: tests, validation, visualization and editing. All authors have read and agreed to the published version of the manuscript.

Funding

This research received no external funding.

Institutional Review Board Statement

Not applicable.

Informed Consent Statement

Not applicable.

Data Availability Statement

Raw data available on request.

Conflicts of Interest

The authors declare no conflict of interest.

Use of AI and AI-Assisted Technologies

No AI tools were utilized for this paper.

References

1. Kurpiel, S.; Zagórski, K.; Cieślik, J.; et al. Evaluation of the Vibration Signal during Milling Vertical Thin-Walled Structures from Aerospace Materials. *Sensors* **2023**, *23*, 6398. https://doi.org/10.3390/s23146398.
2. Kurpiel, S.; Zagórski, K.; Cieślik, J.; et al. Investigation of Selected Surface Topography Parameters and Deformation during Milling of Vertical Thin-Walled Structures from Titanium Alloy Ti6Al4V. *Materials* **2023**, *16*, 3182. https://doi.org/10.3390/ma16083182.
3. Hou, J.; Wang, B.; Lv, D.; et al. Investigation of the Influence of Electrolytic Milling Machining Parameters on the Machining Accuracy of Thin-Walled Parts. *Sci. Rep.* **2024**, *14*, 28288. https://doi.org/10.1038/s41598-024-80052-7.
4. Zablotskyi, V.; Tkachuk, A.; Prozorovskyi, S.; et al. Influence of Turning Operations on Waviness Characteristics of Working Surfaces of Rolling Bearings. In *Advances in Design, Simulation and Manufacturing V*, *Proceedings of the 5th International Conference on Design, Simulation, Manufacturing: The Innovation Exchange, DSMIE-2022, Poznan, Poland, 7–10 June 2022*; Ivanov, V., Trojanowska, J., Pavlenko, I., Eds.; Lecture Notes in Mechanical Engineering; Springer: Cham, Switzerland, 2022; pp. 345–354. https://doi.org/10.1007/978-3-031-06025-0_34.
5. Maes, V.K.; Macquart, T.; Weaver, P.M.; et al. Sensitivity of Cross-Sectional Compliance to Manufacturing Tolerances for Wind Turbine Blades. *Wind Energy Sci.* **2025**, *9*, 165–180. https://doi.org/10.5194/wes-9-165-2025.
6. Kolmakova, D.; Baturin, O.; Popov, G. Effect of Manufacturing Tolerances on the Turbine Blades. In *Proceedings of the ASME 2014 Gas Turbine India Conference*; New Delhi, India, 15–17 December 2014. https://doi.org/10.1115/gtindia2014-8253.
7. Moneta, G.; Jachimowicz, J. Impact of Manufacturing Tolerances on Stress in a Turbine Blade Fir-Tree Root. *Fatigue Aircr. Struct.* **2020**, *12*, 92–101. https://doi.org/10.2478/fas-2020-0009.
8. Zhao, B.; Ding, W.; Shan, Z.; et al. Collaborative Manufacturing Technologies of Structure Shape and Surface Integrity for Complex Thin-Walled Components of Aero-Engine: Status, Challenge, and Tendency. *Chin. J. Aeronaut.* **2023**, *36*, 1–24. https://doi.org/10.1016/j.cja.2023.02.008.
9. Li, Y.; Ding, F.; Tian, W.; et al. Prediction of Modal Parameters for Thin-Walled Blade Milling Process Considering Material Removal Effect. *PLoS ONE* **2025**, *20*, e0323871. https://doi.org/10.1371/journal.pone.0323871.
10. Dyadya, S.; Frolov, M.; Tanchenko, S.; et al. Attendant Free Vibrations and Assessment of Their Influence on the Machined Surface Macrogeometry While End Milling. In *Advances in Design, Simulation and Manufacturing VIII, Proceedings of the 8th International Conference on Design, Simulation, Manufacturing: The Innovation Exchange, DSMIE-2025, Porto, Portugal, 17–20 June 2025*; Ivanov, V., Silva, F., Trojanowska, J., Eds.; Lecture Notes in Mechanical Engineering; Springer: Cham, Switzerland, 2025; pp. 327–337. https://doi.org/10.1007/978-3-031-95211-1_27.
11. Dyadya, S.; Frolov, M.; Tanchenko, S.; et al. Feed Rate Influence Research on the Machined Surface Waviness Parameters in End Up Milling of Thin-Walled Parts. In *Smart Innovations in Energy and Mechanical Systems*; Pavlenko, D., Tryshyn, P., Honchar, N., Eds.; Lecture Notes in Networks and Systems; Springer: Cham, Switzerland, 2025; pp. 79–89. https://doi.org/10.1007/978-3-031-95191-6_8.
12. Kouahla, I.; Yallese, M.A.; Belhadi, S.; et al. Tool Vibration, Surface Roughness, Cutting Power, and Productivity Assessment Using RSM and GRA Approach during Machining of Inconel 718 with PVD-Coated Carbide Tool. *Int. J. Adv. Manuf. Technol.* **2022**, *122*, 1835–1856. https://doi.org/10.1007/s00170-022-09988-2.
13. Wang, X.; Li, S.; Guo, Z.; et al. Research on TA2 Dry/Wet Milling Force–Vibration Characteristics and Vibration Prediction Model. *Noise Vib. Worldw.* **2026**, *57*, 59–67. https://doi.org/10.1177/09574565251382128.
14. Zhao, W.; Liu, X.; Li, R. A Geometric-Matrix Method for Cutting Force Modeling. *Mech. Syst. Signal Process.* **2026**, *242*, 113663. https://doi.org/10.1016/j.ymssp.2025.113663.
15. Dongre, P.; Zoting, J.; Gokhe, D. Exploring Surface Roughness and Tool Vibration through Experimental Investigation and Modeling with EDM-Textured Cutting Tools. In *Recent Advances in Condition Monitoring*; Andhare, A., Ganesh Kumar, P., Eds.; Springer: Singapore, 2024; pp. 221–231. https://doi.org/10.1007/978-981-96-5791-9_23.

16. Ozoegwu, C.G.; Ofochebe, S.M.; Omenyi, S.N. A Method of Improving Chatter-Free Conditions with Combined-Mode Milling. *J. Manuf. Process.* **2016**, *21*, 1–13. https://doi.org/10.1016/j.jmapro.2015.10.008.
17. Yi, J.; Wang, X.; Zhu, Y.; et al. Deformation Control in Mesoscale Micro-Milling of Curved Thin-Walled Structures. *Materials* **2024**, *17*, 5071. https://doi.org/10.3390/ma17205071.
18. Kononenko, S.; Dobrotvorskiy, S.; Basova, Y.; et al. Impact of Overlapping Method on Cutting Forces and Surface Formation in End Milling of Thin-Walled Parts. In *Smart Innovations in Energy and Mechanical Systems*; Pavlenko, D., Tryshyn, P., Honchar, N., Eds.; Lecture Notes in Networks and Systems; Springer: Cham, Switzerland, 2025; pp. 67–78. https://doi.org/10.1007/978-3-031-95191-6_7.
19. Abebe, R.; Gopal, M. Exploring the Effects of Vibration on Surface Roughness during CNC Face Milling on Aluminum 6061-T6 Using Sound Chatter. *Mater. Today Proc.* **2023**, *90*, 43–49. https://doi.org/10.1016/j.matpr.2023.04.332.
20. Sedehi, S.M.R.; Norouzi Palangani, F.; Maleki, Z.; et al. Effect of Conventional and Climb Milling on the Mechanical Properties and Biocompatibility of Pure Titanium; Application of the Williamson-Hall Method. *J. Mod. Process. Manuf. Prod.* **2025**, *17*, 51–61. https://doi.org/10.58209/ijwph.17.1.51.
21. Ciecielag, K.; Skoczylas, A.; Matuszak, J. Measurement of Cutting Forces in Conventional and Climb Milling by Recurrence Analysis. In Proceedings of the 2024 11th International Workshop on Metrology for AeroSpace (MetroAeroSpace), Lublin, Poland, 3–5 June 2024; pp. 531–536. https://doi.org/10.1109/MetroAeroSpace61015.2024.10591550.
22. Lassila, A.A.; Svensson, D.; Wang, W.; et al. Numerical Evaluation of Cutting Strategies for Thin-Walled Parts. *Sci. Rep.* **2024**, *14*, 1459. https://doi.org/10.1038/s41598-024-51883-1.
23. Wang, R.; Sun, Y. Chatter Prediction for Parallel Mirror Milling of Thin-Walled Parts by Dual-Robot Collaborative Machining System. *Robot. Comput. Integr. Manuf.* **2024**, *88*, 102715. https://doi.org/10.1016/j.rcim.2024.102715.
24. Yue, C.; Gao, H.; Liu, X.; et al. A Review of Chatter Vibration Research in Milling. *Chin. J. Aeronaut.* **2019**, *32*, 215–242. https://doi.org/10.1016/j.cja.2018.11.007.
25. McClements, D. Climb Milling vs. Conventional Milling: Their Key Differences. Available online: https://www.xometry.com/resources/machining/climb-milling-vs-conventional-milling/ (accessed on 15 January 2026).
26. Li, X.; Ni, J.; Liu, X.; et al. Chatter-Free Milling of Aerospace Thin-Walled Parts. *J. Mater. Process. Technol.* **2025**, *341*, 118903. https://doi.org/10.1016/j.jmatprotec.2025.118903.
27. Li, Y.W.; Sun, Y.S.; Zhou, X.G. Theoretical Analysis and Experimental Verification that Influence Factors of Climb and Conventional Milling on Surface Roughness. *Appl. Mech. Mater.* **2013**, *459*, 407–412. https://doi.org/10.4028/www.scientific.net/AMM.459.407.
28. Munoa, J.; Beudaert, X.; Dombovari, Z.; et al. Chatter Suppression Techniques in Metal Cutting. *CIRP Ann.* **2016**, *65*, 785–808. https://doi.org/10.1016/j.cirp.2016.06.004.
29. Vnukov, Y.N.; Dyadya, S.I.; Kozlova, E.B.; et al. *Auto Oscillations at Milling of Thin-Walled Elements of the Details*; ZNTU: Zaporizhzhia, Ukraine, 2017.
30. Germashev, A.I.; Byelikov, S.B.; Logominov, V.A. Automation of the Process of Selecting the Milling Modes of Thin-Wall Elements of Parts. *Herald Aeroenginebuild.* **2018**, *1*, 83–89. https://doi.org/10.15588/1727-0219-2018-1-12.
31. Frolov, M.; Dyadya, S.; Tanchenko, S.; et al. Attendant Free Vibrations and Their Role in the Formation of Macrorelief at the End Milling of Thin-Walled Structures When Changing the Radial Depth of Cut. *J. Mech. Eng. Manuf.* **2026**, *2*, 2. https://doi.org/10.53941/jmem.2026.100002.
32. Ramachandran, K.M.; Tsokos, C.P. *Mathematical Statistics with Applications*; Elsevier Academic Press: Amsterdam, The Netherlands, 2009.
33. Stone, B. *Chatter and Machine Tools*; Springer: Cham, Switzerland, 2014. https://doi.org/10.1007/978-3-319-05236-6.